

Guest-induced Modulation of Energy Transfer Process in Porphyrin-based Artificial Light Harvesting Dendrimers

Dajeong Yim, Jooyoung Sung, Serom Kim, Juwon Oh, Hongsik Yoon, Young Mo Sung, Dongho Kim, and Woo-Dong Jang

J. Am. Chem. Soc., **Just Accepted Manuscript** • DOI: 10.1021/jacs.6b11804 • Publication Date (Web): 15 Dec 2016

Downloaded from <http://pubs.acs.org> on December 17, 2016

Just Accepted

“Just Accepted” manuscripts have been peer-reviewed and accepted for publication. They are posted online prior to technical editing, formatting for publication and author proofing. The American Chemical Society provides “Just Accepted” as a free service to the research community to expedite the dissemination of scientific material as soon as possible after acceptance. “Just Accepted” manuscripts appear in full in PDF format accompanied by an HTML abstract. “Just Accepted” manuscripts have been fully peer reviewed, but should not be considered the official version of record. They are accessible to all readers and citable by the Digital Object Identifier (DOI®). “Just Accepted” is an optional service offered to authors. Therefore, the “Just Accepted” Web site may not include all articles that will be published in the journal. After a manuscript is technically edited and formatted, it will be removed from the “Just Accepted” Web site and published as an ASAP article. Note that technical editing may introduce minor changes to the manuscript text and/or graphics which could affect content, and all legal disclaimers and ethical guidelines that apply to the journal pertain. ACS cannot be held responsible for errors or consequences arising from the use of information contained in these “Just Accepted” manuscripts.



Guest-induced Modulation of Energy Transfer Process in Porphyrin-based Artificial Light Harvesting Dendrimers

Dajeong Yim, Jooyoung Sung,[†] Serom Kim, Juwon Oh, Hongsik Yoon, Young Mo Sung, Dongho Kim,^{*} and Woo-Dong Jang^{*}

Department of Chemistry, Yonsei University, 50 Yonsei-ro, Seodaemun-Gu, Seoul 120-749, Korea

porphyrin • energy transfer • host-guest chemistry • photoswitching • fluorescence

ABSTRACT: A series of dendritic multi-porphyrin arrays ($P_{Zn}Tz-nP_{FB}$; $n = 2, 4, 8$) comprising a triazole-bearing focal zinc porphyrin (P_{Zn}) with a different number of freebase porphyrin (P_{FB}) wings has been synthesized and their photoinduced energy transfer process has been evaluated. UV/Vis absorption, emission, and time-resolved fluorescence measurements indicated that efficient excitation energy transfer takes place from the focal P_{Zn} to P_{FB} wings in $P_{Zn}Tz-nP_{FB}$. The triazole-bearing P_{Zn} effectively formed host-guest complexes with anionic species by means of axial coordination with the aid of multiple C-H hydrogen bonds. By addition of various anionic guest to $P_{Zn}Tz$ and $P_{Zn}Tz-nP_{FB}$, strong bathochromic shifts of P_{Zn} absorption were observed, indicating the HOMO-LUMO gap ($\Delta E_{HOMO-LUMO}$) of P_{Zn} decreased by anion binding. Time-resolved fluorescence measurements revealed that the fluorescence emission predominantly takes place from P_{Zn} in $P_{Zn}Tz-nP_{FB}$ after the addition of CN^- . This change was reversible because a treatment with a silver strip to remove CN^- fully recovered the original energy transfer process from the focal P_{Zn} to P_{FB} wings.

INTRODUCTION

Natural photosynthetic systems convert solar energy to chemical energy with extremely high energy conversion efficiency.¹⁻⁹ Photosynthesis is initiated when light is absorbed by light-harvesting antenna complexes (LHCs), which are composed of three-dimensional arrays of a large number of porphyrin derivatives.^{6,9} The elegant architecture of LHCs enables effective light absorption as well as excitation energy transfer to the reaction center.⁷ Such structural uniqueness as well as the extraordinary high energy conversion efficiency offer strong motivations to synthetic chemists upon the molecular designing in photo-functional materials. For example, as the mimicry of LHCs, various types of multi-porphyrin arrays have been synthesized to investigate their light energy transduction.¹⁰⁻¹⁶ Typically, porphyrin-based dendritic architectures have attracted much attention because their gradient structures contributed to the directional energy transfer from periphery to the focal core.^{14,15} Such the directional energy transfer processes would be one of the key factors in the high energy conversion efficiency of natural light harvesting systems.¹⁻⁵ Natural directional energy transfer phenomena have inspired the designs of artificial photofunctional devices, including photovoltaic,¹⁷⁻¹⁹ electroluminescent,^{9,20,21} and biomedical devices.²²⁻²⁶ Although directed energy transfer can be achieved by simple conjugation of donor-acceptor pairs, natural photosynthetic systems involve much more complicated mechanisms than artificial ones

for the precise regulation of light-energy conversion processes. LHCs possess various molecular accessories for the regulation of energy transduction by the formation of supramolecular complexes with specific proteins or ionic species.^{4,27-29} The binding of molecular accessories to LHCs can turn on or off the major function of light harvesting. For example, under strong sun light condition, plants modulate their energy transfer pathways to protect their light harvesting system from photo-damage.⁴

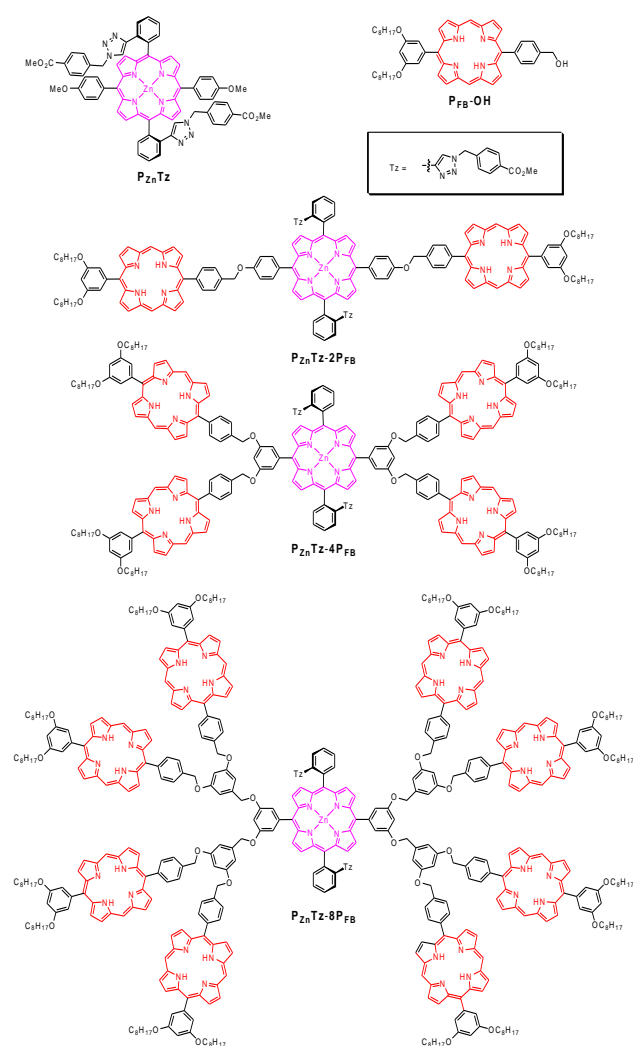
We recently reported porphyrin-based molecular tweezers with a bisindole bridge, which exhibits excellent switching of energy transfer direction in response to the coordination of a metal ion with the bisindole bridge.³⁰ Using this metal-bisindole coordination process, we have controlled the energy transfer process between two heterogeneous systems, namely a zinc porphyrin and the bisindole bridge.

In the present study, we attempted to develop a new artificial light harvesting dendritic multiporphyrin arrays in which guest binding to the center of dendritic architecture can modulate the energy transfer process. A series of multiporphyrin dendrimers ($P_{Zn}Tz-nP_{FB}$; $n = 2, 4, 8$, Chart 1), composed of a triazole-bearing focal zinc porphyrin (P_{Zn}) with a different number of freebase porphyrin (P_{FB}) wings, was synthesized and their photoinduced energy transfer process was evaluated. Structural fragments of $P_{Zn}Tz-nP_{FB}$, namely, $P_{Zn}Tz$ and $P_{FB}-OH$, were also prepared for control experiments (Chart 1).

EXPERIMENTAL SECTION

Materials and Measurements. All commercially available reagents were reagent grade and used without further purification. Dichloromethane (CH_2Cl_2) and tetrahydrofuran (THF) were freshly distilled before each use. All anions were used as a form of tetrabutylammonium salt, which have used as received from Sigma-Aldrich. Steady-state electronic absorption spectra and fluorescence emission spectra were on a JASCO V-660 and JASCO FP-6300 spectrometers, respectively. All steady-state measurements were carried out by using a quartz cuvette with a path length of 1 cm at ambient temperatures. ^1H and ^{13}C NMR spectra were recorded on a Bruker Advance DPX 250, DPX 400 spectrometer at 25 °C in CDCl_3 , $\text{THF-}d_8$, and $\text{DMSO-}d_6$. MALDI-TOF-MS was performed on Bruker Daltonics LRF20 with dithranol (1,8,9-trihydroxyanthracene) as the matrix. Recycling SEC was performed on JAI model LC9021 equipped with JAIGEL-1H, JAIGEL-2H and JAIGEL-3H columns using CHCl_3 (J. T. Baker) as the eluent. Analytical SEC was performed on a JASCO HPLC equipped with HF-403HQ and HF-404HQ columns (Shodex, Tokyo, Japan) using THF as the eluent.

CHART 1. Chemical structures of multi-porphyrin dendrimers ($\text{P}_{\text{Zn}}\text{Tz-}n\text{P}_{\text{FB}}$) and their structural fragments ($\text{P}_{\text{Zn}}\text{Tz}$ and $\text{P}_{\text{FB}}\text{-OH}$).

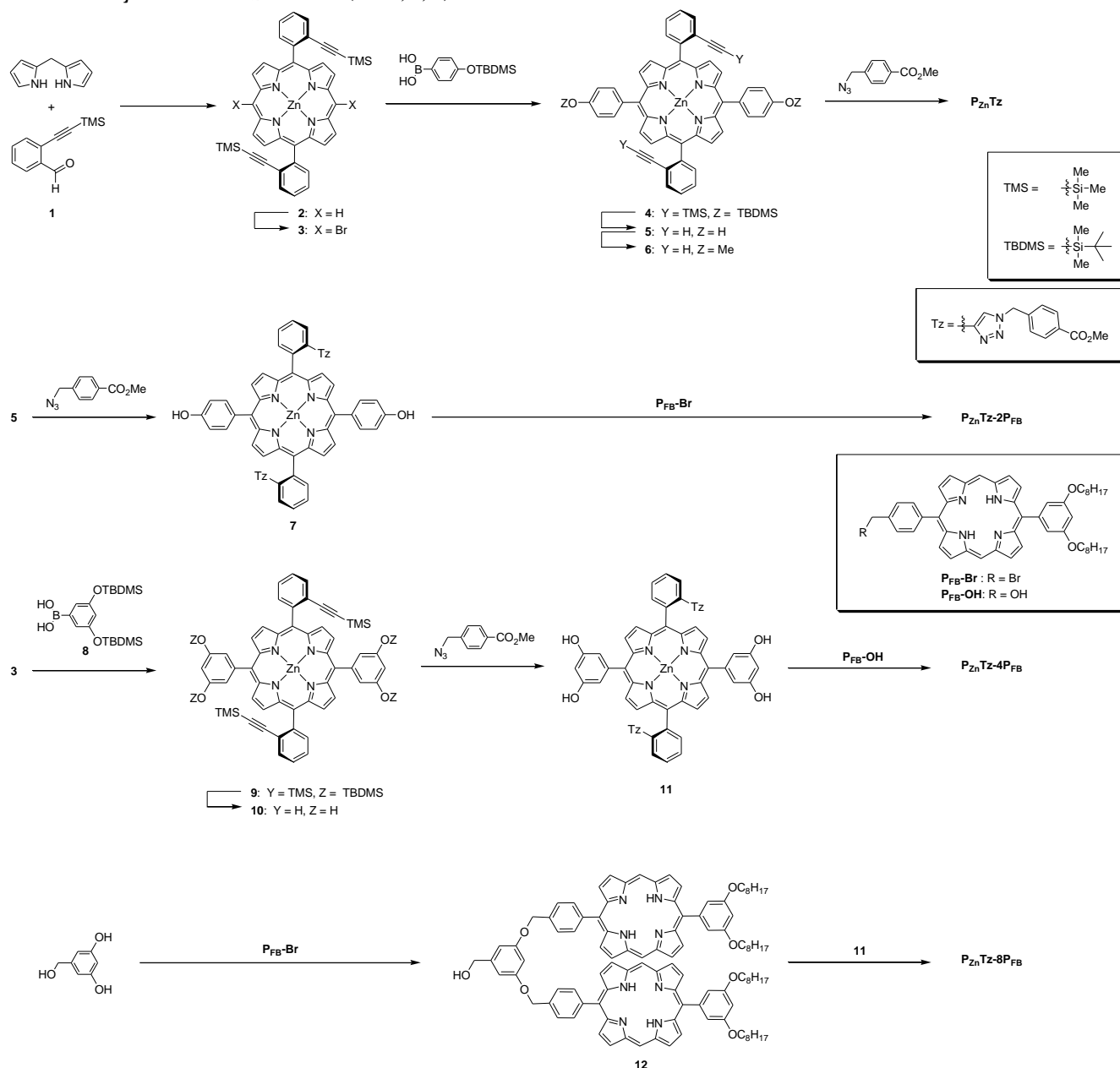


Time Correlated Single Photon Counting Measurement. Time-resolved fluorescence lifetime experiments were performed by the time-correlated single-photon-counting (TCSPC) technique. As an excitation light source, we used a Ti:sapphire laser (Mai Tai BB, Spectra-Physics) which provides a repetition rate of 800 kHz with ~ 100 fs pulses generated by a homemade pulse-picker. The output pulse of the laser was frequency-doubled by a 1 mm thickness of a second harmonic crystal (β -barium borate, BBO, CASIX). The fluorescence was collected by a microchannel plate photomultiplier (MCP-PMT, Hamamatsu, R3809U-15) with a thermoelectric cooler (Hamamatsu, C4878) connected to a TCSPC board (Becker & Hickel SPC-130). The overall instrumental response function was about 25 ps (the full width at half maximum (fwhm)). A vertically polarized pump pulse by a Glan-laser polarizer was irradiated to samples, and a sheet polarizer, set at an angle complementary to the magic angle (54.7°), was placed in the fluorescence collection path to obtain polarization-independent fluorescence decays.

Computational Method. Quantum mechanical calculation was performed with the Gaussian 09 program suite.³¹ All calculations were carried out by the density functional theory (DFT) method with Becke's three-parameter hybrid exchange functional and the Lee-Yang-Parr correlation functional (B3LYP), employing the 6-31G(d,p) basis set.^{32,33} The oscillator strength was calculated by performing time dependent (TD)-DFT calculation.

Synthesis. The synthetic procedure of $\text{P}_{\text{Zn}}\text{Tz}$ and $\text{P}_{\text{Zn}}\text{Tz-}n\text{P}_{\text{FB}}$ are outlined in Scheme 1. Hydroxy-group-bearing porphyrin ($\text{P}_{\text{FB}}\text{-OH}$), bromide-bearing porphyrin ($\text{P}_{\text{FB}}\text{-Br}$), dipyrromethane, and 2-((trimethylsilyl)ethynyl)benzaldehyde (**1**) were synthesized according to the literature procedure.³⁴⁻³⁶ The synthetic procedures of compounds **2-11** are shown in supporting information.

$\text{P}_{\text{Zn}}\text{Tz}$: $\text{CuSO}_4 \cdot 5\text{H}_2\text{O}$ (479 mg, 1.9 mmol) and sodium ascorbate (373 mg, 1.9 mmol) were added to a mixture of **6** (148 mg, 0.19 mmol) and methyl 4-(azidomethyl)benzoate (310 mg, 0.94 mmol) in 20 mL THF/ H_2O (1:1). The reaction mixture was stirred for 5 h at 50 °C, and then poured into CH_2Cl_2 (100 mL). The organic layer was separated. After evaporation of the solvent under reduced pressure, the residue was purified using column chromatography with 1% MeOH/ CH_2Cl_2 as the eluent to give $\text{P}_{\text{Zn}}\text{Tz}$ as a purple powder (147 mg, 67%): ^1H NMR (400 MHz, $\text{DMSO-}d_6$, 25 °C) δ = 8.75-8.74 (d, 4 H, J = 4.0 Hz), 8.63-8.62 (d, 4 H, J = 4.0 Hz), 8.59-8.57 (d, 2 H, J = 8.0 Hz), 8.13-8.11 (d, 2 H, J = 8.0 Hz), 8.01-7.99 (d, 4 H, J = 8.0 Hz), 7.97-7.95 (t, 2 H, J = 8.0 Hz), 7.80-7.78 (t, 2 H, J = 8.0 Hz), 7.33-7.31 (d, 4 H, J = 8.0 Hz), 7.03-7.01 (d, 4 H, J = 8.4 Hz), 5.72-5.70 (d, 4 H, J = 8.4 Hz), 4.71 (s, 2 H), 4.40 (s, 4 H), 4.04 (s, 6 H), 3.78 (s, 6 H). ^{13}C NMR (100 MHz, CDCl_3 , 25 °C) δ = 165.82, 159.52, 150.90, 149.88, 147.52, 139.94, 138.60, 135.64, 134.93, 134.60, 132.93, 131.57, 129.14, 129.03, 128.54, 127.47, 126.68, 125.76, 122.07, 121.17, 119.40, 112.43, 55.77, 52.22, 51.98, 0.21. MALDI-TOF-MS: m/z : calcd. for $\text{C}_{68}\text{H}_{50}\text{N}_{10}\text{O}_6\text{Zn}$: 1168.57 [M]⁺; found 1166.60.

Scheme 1. Synthesis of $P_{Zn}Tz-nP_{FB}$ ($n = 2, 4, 8$)

$P_{Zn}Tz-2P_{FB}$: A dry THF solution (6 mL) of **7** (60 mg, 0.0525 mmol), P_{FB-Br} (90 mg, 0.110 mmol), K_2CO_3 (29 mg, 0.210 mmol), and 18-crown-6 ether (1.4 mg, 0.00525 mmol) was refluxed under N_2 for 14 h, and subsequently evaporated. The residue was dissolved in CH_2Cl_2 (100 mL) and washed with water (100 mL x 3), and evaporated. The residue was chromatographed on silica gel using 1% MeOH/ CH_2Cl_2 as the eluent, and the product was collected, evaporated to dryness, and freeze-dried with benzene to give $P_{Zn}Tz-2P_{FB}$ as a purple powder in 87% yield (119.1 mg): 1H NMR (400 MHz, $CDCl_3$, 25 °C) δ = 10.35 (s, 4 H), 9.45–9.41 (m, 8 H), 9.23–9.22 (d, 4 H, J = 4.8 Hz), 9.19–9.18 (d, 4 H, J = 4.8 Hz), 9.06–9.05 (d, 4 H, J = 4.0 Hz), 8.93–8.92 (d, 4 H, J = 4.0 Hz), 8.75–8.73 (d, 2 H, J = 8.0 Hz), 8.43–8.41 (d, 4

H, J = 8.0 Hz), 8.21–8.19 (d, 4 H, J = 8.4 Hz), 8.19–8.17 (d, 2 H, J = 8.0 Hz), 8.11–8.09 (d, 4 H, J = 8.0 Hz), 8.00–7.96 (t, 2 H, J = 8.0 Hz), 7.79–7.75 (t, 2 H, J = 8.0 Hz), 7.63–7.60 (d, 4 H, J = 8.4 Hz), 7.44 (s, 4 H), 6.94–6.92 (m, 6 H), 5.76–5.74 (m, 8 H), 4.55 (s, 2 H), 4.30 (s, 4 H), 4.19–4.15 (t, 8 H, J = 8.0 Hz), 3.78 (s, 6 H), 1.93–1.86 (m, 8 H), 1.42–1.25 (m, 40 H), 0.89–0.86 (t, 12 H, J = 4.0 Hz), -3.11 (s, 4 H). ^{13}C NMR (100 MHz, $CDCl_3$, 25 °C) δ = 165.94, 159.06, 158.80, 151.05, 150.10, 147.73, 147.26, 145.55, 145.39, 143.24, 141.57, 140.01, 138.73, 136.65, 135.90, 135.40, 135.07, 133.11, 131.93, 131.84, 131.47, 131.20, 129.30, 127.70, 126.83, 126.71, 125.94, 122.17, 121.31, 119.70, 119.32, 118.80, 114.75, 113.63, 105.55, 101.10, 70.71, 52.40, 52.22, 32.04, 29.64, 29.48, 26.36, 22.89, 14.34, 0.22. MALDI-

TOF-MS: m/z : calcd. for $C_{164}H_{154}N_{18}O_{10}Zn$: 2602.47 [M]⁺; found 2599.77.

P_{Zn}Tz-4P_{FB}: A dry THF solution (1 mL) in a schlenk tube of **11** (57 mg, 0.049 mmol), **P_{FB}-OH** (154 mg, 0.21 mmol), and PPh₃ (54 mg, 0.21 mmol) was stirred at 0 °C under N₂ for 30 min, and 0.11 mL (40% in toluene 1.9 M, 0.21 mmol) of DEAD was added to the reaction mixture at 0 °C. After stirring for 12 h, the mixture solution was washed with water (100 mL) and the organic layer was evaporated in vacuo. The residue was purified by column chromatography with 1% MeOH/CH₂Cl₂ and recycling SEC with CHCl₃ as the eluent. Then, after short column chromatography, **P_{Zn}Tz-4P_{FB}** was obtained by recrystallization as a reddish powder: ¹H NMR (400 MHz, CDCl₃, 25 °C) δ = 10.24 (s, 8 H), 9.37-9.36 (d, 8 H, J = 4.4 Hz), 9.28-9.27 (d, 8 H, J = 4.4 Hz), 9.25-9.24 (d, 4 H, J = 4.8 Hz), 9.21-9.20 (d, 8 H, J = 4.8 Hz), 9.09-9.08 (d, 8 H, J = 4.4 Hz), 8.97-8.95 (d, 4 H, J = 4.4 Hz), 8.31-8.29 (m, 10 H), 8.09-8.07 (d, 2 H, J = 7.6 Hz), 7.97-7.95 (d, 8 H, J = 7.6 Hz), 7.80 (s, 4 H), 7.51 (s, 2 H), 7.44-7.43 (d, 8 H, J = 2.0 Hz), 7.43-7.41 (d, 2 H, J = 7.6 Hz), 7.39-7.35 (t, 2 H, J = 6.8 Hz), 6.93-6.92 (t, 4 H, J = 2.0 Hz), 6.75-6.73 (d, 4 H, J = 8.0 Hz), 5.67-5.63 (m, 8 H), 4.69 (s, 2 H), 4.16-4.10 (m, 24 H), 3.64 (s, 6 H), 1.91-1.84 (m, 16 H), 1.53-1.46 (m, 16 H), 1.39-1.25 (m, 64 H), 0.88-0.85 (t, 24 H, J = 6.8 Hz), -3.13 (s, 8 H). ¹³C NMR (100 MHz, CDCl₃, 25 °C) δ = 170.99, 165.74, 158.82, 158.52, 150.50, 150.38, 147.77, 147.31, 147.18, 145.50, 145.36, 144.69, 143.25, 141.47, 140.03, 138.48, 136.59, 135.39, 133.11, 133.08, 133.03, 132.15, 132.08, 132.05, 131.85, 131.43, 131.10, 129.44, 129.21, 126.60, 126.16, 122.09, 121.20, 119.86, 119.32, 118.74, 115.80, 115.75, 115.69, 114.88, 114.85, 114.79, 114.72, 105.50, 101.19, 77.44, 70.70, 68.63, 52.26, 32.03, 29.93, 29.62, 29.46, 26.35, 22.87, 14.31, 0.22. MALDI-TOF-MS: m/z : calcd. for $C_{262}H_{262}N_{26}O_{16}Zn$: 4096.43 [M]⁺; found 4096.76.

12: 3,5-Dihydroxy benzyl alcohol (83.8 mg, 0.59 mmol), **P_{FB}-Br** (990 mg, 1.2 mmol), K₂CO₃ (411 mg, 3.0 mmol), and 18-crown-6-ether were mixed in a 100 mL two-neck round bottomed flask. The flask was degassed under high vacuum and back-filled with N₂. Acetone (9 mL) and dry DMF (3 mL) were added under nitrogen. The reaction mixture was refluxed for 12 h. The solution was quenched with water and removed acetone. The mixture was dissolved in CH₂Cl₂ and washed with water. The organic layer was separated. After evaporation of the solvent under reduced pressure, the residue was purified using column chromatography with CH₂Cl₂ to give **12** (860.4 mg, 90%): ¹H NMR (400 MHz, CDCl₃, 25 °C) δ = 10.30 (s, 4 H), 9.40-9.39 (d, 4 H, J = 4.8 Hz), 9.38-9.37 (d, 4 H, J = 4.4 Hz), 9.20-9.19 (d, 4 H, J = 4.8 Hz), 9.14-9.13 (d, 4 H, J = 4.4 Hz), 8.37-8.35 (d, 4 H, J = 8.0 Hz), 7.97-7.95 (d, 4 H, J = 8.0 Hz), 7.44-7.43 (d, 4 H, J = 2.0 Hz), 7.03-7.02 (d, 1 H, J = 2.0 Hz), 6.99-6.98 (d, 2 H, J = 2.0 Hz), 6.93-6.92 (t, 2 H, J = 2.0 Hz), 5.55 (s, 4 H), 4.89-4.87 (d, 2 H, J = 6.0 Hz), 4.18-4.14 (t, 8 H, J = 8.0 Hz), 1.89-1.83 (m, 8 H), 1.54-1.48 (m, 8 H), 1.40-1.28 (m, 32 H), 0.88-0.85 (t, 12 H, J = 6.4 Hz), -3.11 (d, 4 H). MALDI-TOF-MS: m/z : calcd. for $C_{105}H_{116}N_8O_7$: 1602.09 [M]⁺; found 1602.28.

P_{Zn}Tz-8P_{FB}: A dry THF solution (2 mL) in a schlenk tube of **11** (29 mg, 0.025 mmol), **12** (158.2 mg, 0.099 mmol), and PPh₃ (25.9 mg, 0.099 mmol) was stirred at 0 °C under N₂ for 30 min, and 0.05 mL (40% in toluene 1.9 M, 0.099 mmol)

of DIAD was added to the reaction mixture at 0 °C. Then after stirring for 12 h, the mixture solution was washed with water (100 mL) and the organic layer was evaporated in vacuo. The residue was purified by column chromatography with EtOAc/CH₂Cl₂ and recycling SEC with CHCl₃ as the eluent. **P_{Zn}Tz-8P_{FB}** was obtained as a purple solid: ¹H NMR (400 MHz, CDCl₃, 25 °C) δ = 9.98 (s, 16 H), 9.22-9.20 (d, 4 H, J = 4.0 Hz), 9.17-9.16 (d, 16 H, J = 4.0 Hz), 9.12-9.11 (d, 16 H, J = 4.0 Hz), 9.05-9.04 (d, 16 H, J = 4.0 Hz), 8.91-8.90 (d, 16 H, J = 4.0 Hz), 8.87-8.86 (d, 4 H, J = 4.0 Hz), 8.43-8.41 (d, 2 H, J = 8.0 Hz), 8.10-8.08 (d, 16 H, J = 8.0 Hz), 7.94-7.92 (d, 2 H, J = 8.0 Hz), 7.77-7.73 (t, 2 H, J = 8.0 Hz), 7.72 (s, 4 H), 7.69-7.67 (d, 16 H, J = 8.0 Hz), 7.61-7.57 (t, 2 H, J = 8.0 Hz), 7.38 (s, 4 H), 7.37 (s, 20 H), 6.97 (s, 8 H), 6.93 (s, 4 H), 6.88 (s, 10 H), 6.34-5.32 (d, 4 H, J = 8.0 Hz), 5.34 (s, 16 H), 5.01-4.99 (d, 4 H, J = 8.0 Hz), 4.63 (s, 2 H), 4.09-4.05 (t, 32 H, J = 6.4 Hz), 3.52 (s, 6 H), 3.41 (s, 4 H), 1.82-1.79 (m, 32 H), 1.48-1.40 (m, 32 H), 1.25-1.23 (m, 128 H), 0.84-0.81 (m, 48 H), -3.27 (s, 16 H). MALDI-TOF-MS: m/z : calcd. for $C_{486}H_{502}N_{42}O_{32}Zn$: 7508.83 [M]⁺; found 7513.75.

RESULT AND DISCUSSION

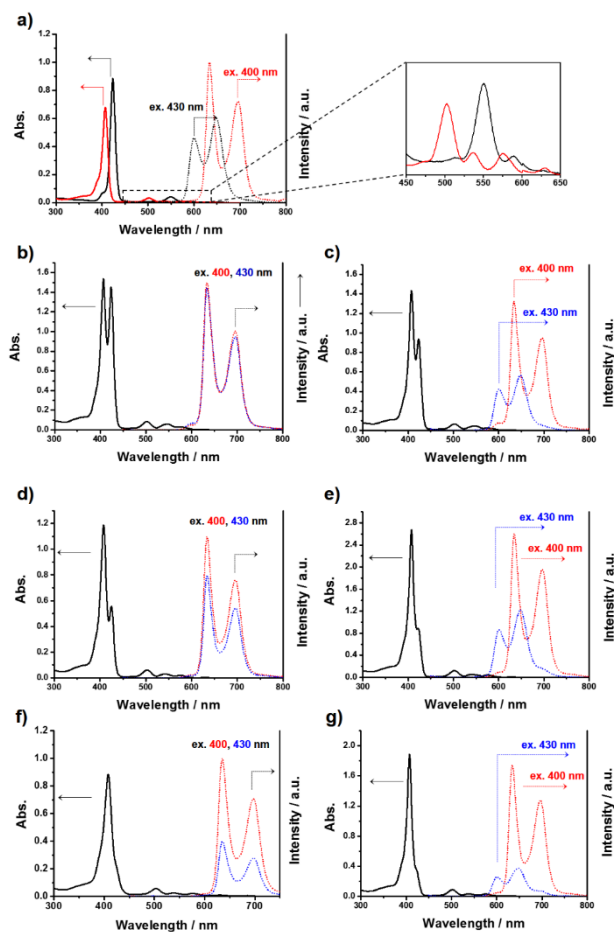
Absorption and emission spectra of all the compounds studied here were acquired in CH₂Cl₂: **P_{Zn}Tz**, **P_{FB}-OH**, **P_{Zn}Tz-*n*P_{FB}S**, and 1:*n* mixtures of **P_{Zn}Tz** and **P_{FB}-OH** (**P_{Zn}Tz/*n*P_{FB}-OH**) as noncovalent references for **P_{Zn}Tz-*n*P_{FB}** (Figure 1). **P_{Zn}Tz** exhibited a strong Soret absorption peak at 423.5 nm and two Q-band absorption peaks at 550.5 and 589.5 nm. The Soret absorption peak of **P_{FB}-OH** appeared at 407.5 nm, a slightly shorter wavelength region than that of **P_{Zn}Tz**. The Q-band absorptions of **P_{FB}-OH** appeared at 502.5, 536.5, 575.0, and 630.0 nm. The lowest excitation energy of **P_{FB}-OH** was slightly smaller than that of **P_{Zn}Tz**. Because the emission band of **P_{Zn}Tz** overlaps with the absorption band of **P_{FB}**, the excitation energy of the focal **P_{Zn}** unit is expected to transfer efficiently to the **P_{FB}** wings.

As expected, the fluorescence emissions of **P_{Zn}Tz-*n*P_{FB}** and **P_{Zn}Tz/*n*P_{FB}-OH** differed considerably. Upon 400 nm excitation, corresponding to the absorption of **P_{FB}**, **P_{Zn}Tz/*n*P_{FB}-OH** exhibited emission peaks at 634.0 and 696.0 nm, consistent with the emission of **P_{FB}-OH** alone. Upon excitation at 430 nm, corresponding to the absorption of **P_{Zn}**, **P_{Zn}Tz/*n*P_{FB}-OH** exhibited emission peaks at 600.5 and 648.0 nm, consistent with the emission of **P_{Zn}** alone. In sharp contrast, **P_{Zn}Tz-*n*P_{FB}** exhibited emission peaks at 634.0 and 696.0 nm, being well matched with the emission of **P_{FB}-OH** (Figure 1 and Table 2). Notably, the shape of the emission spectrum was not varied by changing the excitation wavelength, reflecting efficient energy transfer from **P_{Zn}** to **P_{FB}**. Therefore, when we excite the focal **P_{Zn}** unit in **P_{Zn}Tz-*n*P_{FB}**, the emission takes place predominantly from **P_{FB}** wings.

P_{Zn}Tz can effectively form host-guest complexes with anionic species by means of axial coordination with the aid of multiple C-H hydrogen bonds provided by triazole groups.³⁵⁻³⁸ Table 1 summarizes the association constants for associations between various anionic species and **P_{Zn}Tz**. Binding of F⁻, N₃⁻, and CN⁻ to **P_{Zn}Tz** was typically strong.

1
2
3
4
5
6
7
8
9
10
11
12
13
14
15
16
17
18
19
20
21
22
23
24
25
26
27
28
29
30
31
32
33
34
35
36
37
38
39
40
41
42
43
44
45
46
47
48
49
50
51
52

Axial coordination of guest species onto the porphyrin induces bathochromic shifts in the absorption spectra, the degree of which depends on the electron-donating ability of the guest species: $\text{CN}^- > \text{N}_3^- > \text{Cl}^- > \text{F}^- > \text{AcO}^-$ (Figure 2). The addition of I^- and Br^- led to an appearance of shoulders in the absorption spectra, but saturated binding by these weakly binding guest species would require that they should be present in large excess. Absorption spectrum of $\text{P}_{\text{Zn}}\text{Tz}$ ($2.0 \mu\text{M}$ in CH_2Cl_2) exhibited strong bathochromic shifts with clear isosbestic points by addition of CN^- in the form of tetrabutylammonium salt (Figure S1).³⁹ ^1H NMR spectrum of $\text{P}_{\text{Zn}}\text{Tz}$ showed downfield shift of triazole protons by addition of CN^- (Figure S2). The continuous variation method (Job's plot) indicated the formation of 1:1 host-guest complexes (Figure S1). The bathochromic shift again confirmed the CN^- binding in $\text{P}_{\text{Zn}}\text{Tz}$ - $n\text{P}_{\text{FB}}$ (S4, and S5). The addition of anionic guests caused the absorption originating from the focal P_{Zn} to shift to long-wavelength regions, whereas the peaks originating from the P_{FB} wings did not change at all.



53
54
55
56
57
58
59
60

Figure 1. Absorption (solid line) and fluorescence (dotted line) spectra of a) $\text{P}_{\text{FB}}\text{-OH}$ (red, $2.0 \mu\text{M}$) and $\text{P}_{\text{Zn}}\text{Tz}$ (black, $2.0 \mu\text{M}$), b) $\text{P}_{\text{Zn}}\text{Tz}$ - 2P_{FB} ($2.0 \mu\text{M}$), c) $\text{P}_{\text{Zn}}\text{Tz}$ / $2\text{P}_{\text{FB}}\text{-OH}$ ($2.0 \mu\text{M}$ of $\text{P}_{\text{Zn}}\text{Tz}$), d) $\text{P}_{\text{Zn}}\text{Tz}$ - 4P_{FB} ($1.0 \mu\text{M}$), e) $\text{P}_{\text{Zn}}\text{Tz}$ / $4\text{P}_{\text{FB}}\text{-OH}$ ($1.0 \mu\text{M}$ of $\text{P}_{\text{Zn}}\text{Tz}$), f) $\text{P}_{\text{Zn}}\text{Tz}$ - 8P_{FB} ($0.5 \mu\text{M}$), g) $\text{P}_{\text{Zn}}\text{Tz}$ / $8\text{P}_{\text{FB}}\text{-OH}$ ($0.5 \mu\text{M}$ of $\text{P}_{\text{Zn}}\text{Tz}$) in CH_2Cl_2 , where $\lambda_{\text{ex}} = 400$ (red) and 430 nm (blue).

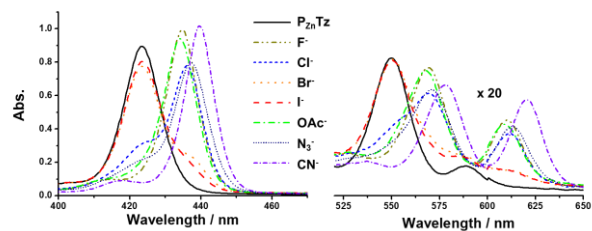


Figure 2. UV-Vis response of $\text{P}_{\text{Zn}}\text{Tz}$ ($2 \mu\text{M}$) to various anions (10 eq.) in CH_2Cl_2 .

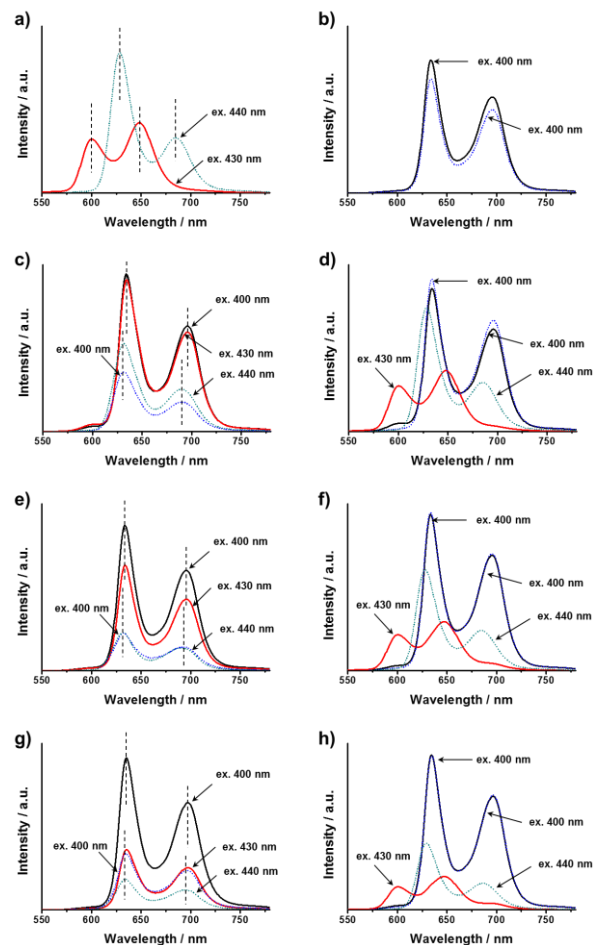


Figure 3. Fluorescence spectra changes without CN^- (solid line) and with CN^- (dotted line) in CH_2Cl_2 . a) $\text{P}_{\text{Zn}}\text{Tz}$ ($2 \mu\text{M}$); b) $\text{P}_{\text{FB}}\text{-OH}$ ($2 \mu\text{M}$); c) $\text{P}_{\text{Zn}}\text{Tz}$ - 2P_{FB} ($2 \mu\text{M}$); d) $\text{P}_{\text{Zn}}\text{Tz}$ / $2\text{P}_{\text{FB}}\text{-OH}$ ($1:2$ mixture) ($2 \mu\text{M}$); e) $\text{P}_{\text{Zn}}\text{Tz}$ - 4P_{FB} ($1 \mu\text{M}$); f) $\text{P}_{\text{Zn}}\text{Tz}$ / $4\text{P}_{\text{FB}}\text{-OH}$ ($1:4$ mixture) ($1 \mu\text{M}$); g) $\text{P}_{\text{Zn}}\text{Tz}$ - 8P_{FB} ($0.5 \mu\text{M}$); h) $\text{P}_{\text{Zn}}\text{Tz}$ / $8\text{P}_{\text{FB}}\text{-OH}$ ($1:8$ mixture) ($0.5 \mu\text{M}$). $\lambda_{\text{ex}} = 400, 430$ and 440 nm. $[\text{CN}^-]/[\text{Host}] = 10 \text{ eq.}$

Table 1. Association constants K for the complex formation of $\text{P}_{\text{Zn}}\text{Tz}$ ^[a] with various anionic guests^[b] at 298 K in CH_2Cl_2 .

Anion	F^-	Cl^-	Br^-	I^-	OAc^-	N_3^-	CN^-
$K/10^5$	10.2	4.06	0.21	0.02	6.46	7.46	15.3

[a] The concentration of $\text{P}_{\text{Zn}}\text{Tz}$ was $2.0 \mu\text{M}$. [b] All guests were in the form of tetrabutylammonium salts.

Because absorption shifts indicate changes in the HOMO–LUMO gap ($\Delta E_{\text{HOMO-LUMO}}$), the binding of anionic guests may influence the energy transfer process in $\text{P}_{\text{Zn}}\text{Tz}-n\text{P}_{\text{FB}}$. The bathochromic shift of the focal P_{Zn} unit in $\text{P}_{\text{Zn}}\text{Tz}-n\text{P}_{\text{FB}}$ indicates decreased $\Delta E_{\text{HOMO-LUMO}}$. If the $\Delta E_{\text{HOMO-LUMO}}$ of the focal P_{Zn} unit becomes smaller than that of the P_{FB} wings, the energy transfer should take place from P_{FB} wings to the focal $\text{P}_{\text{Zn}}\text{Tz}$ unit. Because the greatest bathochromic shift of $\text{P}_{\text{Zn}}\text{Tz}$ occurred by CN^- addition, we investigated the influence of CN^- coordination to the focal P_{Zn} unit on the vertical transition energy and $\Delta E_{\text{HOMO-LUMO}}$ by using DFT calculations at the B3LYP/6-31g(d,p) level based on geometry-optimized structures (Figure S6). The calculated $\Delta E_{\text{HOMO-LUMO}}$ of $\text{P}_{\text{Zn}}\text{Tz}$ (2.82 eV) was slightly larger than that of P_{FB} (2.76 eV). However, the $\Delta E_{\text{HOMO-LUMO}}$ of $\text{P}_{\text{Zn}}\text{Tz}$ became smaller than that of P_{FB} upon coordination with CN^- (2.64 eV), reinforcing our hypothesis that the energy transfer direction can be reversed by addition of CN^- .

Table 2. Wavelengths of fluorescent emission of $\text{P}_{\text{Zn}}\text{Tz}$, $\text{P}_{\text{FB}}\text{-OH}$, $\text{P}_{\text{Zn}}\text{Tz}-n\text{P}_{\text{FB}}$, and $\text{P}_{\text{Zn}}\text{Tz}/n\text{P}_{\text{FB}}\text{-OH}$.

	Without CN^-		With CN^-	
	400 ^[a]	430	400	440
$\text{P}_{\text{Zn}}\text{Tz}$	-	600.5, ^[b] 648.5	-	628.5, 685.0
$\text{P}_{\text{FB}}\text{-OH}$	634.0, 696.0	-	634.0, 696.0	-
$\text{P}_{\text{Zn}}\text{Tz}-2\text{P}_{\text{FB}}$	634.0, 696.0	634.0, 696.0	631.5, 689.5	631.5, 689.5
$\text{P}_{\text{Zn}}\text{Tz}-4\text{P}_{\text{FB}}$	634.0, 696.0	634.0, 696.0	632.0, 690.5	632.0, 690.5
$\text{P}_{\text{Zn}}\text{Tz}-8\text{P}_{\text{FB}}$	635.0, 697.0	635.0, 697.0	634.0, 696.0	634.0, 696.0
$\text{P}_{\text{Zn}}\text{Tz}/2\text{P}_{\text{FB}}\text{-OH}$	634.0, 696.0	600.5, 648.0	634.0, 696.0	628.5, 685.0
$\text{P}_{\text{Zn}}\text{Tz}/4\text{P}_{\text{FB}}\text{-OH}$	633.5, 695.5	600.5, 649.0	633.5, 695.5	628.0, 685.0
$\text{P}_{\text{Zn}}\text{Tz}/8\text{P}_{\text{FB}}\text{-OH}$	633.5, 695.5	600.5, 647.0	634.5, 696.5	629.0, 686.5

[a] λ_{ex} / nm. [b] λ_{em} / nm.

Fluorescence spectra of $\text{P}_{\text{Zn}}\text{Tz}$, $\text{P}_{\text{FB}}\text{-OH}$, $\text{P}_{\text{Zn}}\text{Tz}-n\text{P}_{\text{FB}}$, and $\text{P}_{\text{Zn}}\text{Tz}/n\text{P}_{\text{FB}}\text{-OH}$ were measured again in the presence of CN^- (10.0 eq) (Figure 3). Figure 3 shows the spectral changes of $\text{P}_{\text{Zn}}\text{Tz}-2\text{P}_{\text{FB}}$ and $\text{P}_{\text{Zn}}\text{Tz}/2\text{P}_{\text{FB}}\text{-OH}$ emission by the addition of CN^- . The emission peaks of $\text{P}_{\text{Zn}}\text{Tz}$, originally observed at 600.5 and 648.0 nm, were shifted to 628.5 and 685.0 nm by the addition of CN^- , again indicating the reduced $\Delta E_{\text{HOMO-LUMO}}$. In contrast, the emission bands of $\text{P}_{\text{FB}}\text{-OH}$, observed at 634.0 and 696.0 nm, were not changed at all regardless of the addition of CN^- (Table 2). For the case of $\text{P}_{\text{Zn}}\text{Tz}-2\text{P}_{\text{FB}}$, while its emission spectrum coincided with that of $\text{P}_{\text{FB}}\text{-OH}$ without CN^- addition, the emission bands of $\text{P}_{\text{Zn}}\text{Tz}-2\text{P}_{\text{FB}}$ were slightly hypsochromically shifted and decreased in intensity upon the addition of CN^- . Similar features were observed for $\text{P}_{\text{Zn}}\text{Tz}-4\text{P}_{\text{FB}}$ and $\text{P}_{\text{Zn}}\text{Tz}-8\text{P}_{\text{FB}}$ (Figure 3). Here, the emission spectra of $\text{P}_{\text{Zn}}\text{Tz}-n\text{P}_{\text{FB}}$ with CN^- addition corresponded to that of the CN^- complex of

$\text{P}_{\text{Zn}}\text{Tz}$, indicating that the addition of CN^- causes energy transfer from P_{FB} to P_{Zn} to take place in $\text{P}_{\text{Zn}}\text{Tz}-n\text{P}_{\text{FB}}$.

To investigate quantitatively the energy transfer dynamics in $\text{P}_{\text{Zn}}\text{Tz}-n\text{P}_{\text{FB}}$, time-resolved fluorescence decay profiles were obtained by time-correlated single photon counting technique. The fluorescence decay profile of $\text{P}_{\text{Zn}}\text{Tz}$ was fitted well by the time constant of 1.7 ns, a similar singlet state lifetime of 5,10,15,20-tetrakis aryl zinc porphyrin. $\text{P}_{\text{FB}}\text{-OH}$ exhibited a single exponential decay profile with a time constant of 8.2 ns, a slightly shorter singlet state lifetime than that of 5,10,15,20-tetrakis aryl freebase porphyrin.⁴⁰ Interestingly, whether the P_{FB} wings or the focal P_{Zn} moieties were excited selectively, the fluorescence decay profiles of $\text{P}_{\text{Zn}}\text{Tz}-2\text{P}_{\text{FB}}$ showed the same singlet state lifetimes of 8.2 ns (Figure 4 and Table 3). No short decay component arising from the singlet state of the P_{Zn} moieties was observed, indicating efficient intramolecular energy transfer from P_{Zn} to P_{FB} moieties in $\text{P}_{\text{Zn}}\text{Tz}-2\text{P}_{\text{FB}}$. Similarly, $\text{P}_{\text{Zn}}\text{Tz}-4\text{P}_{\text{FB}}$ also showed only the singlet state lifetime of 8.3 ns indicating efficient energy transfer from P_{Zn} to P_{FB} moieties (Figure 5). The fluorescence decay curve of $\text{P}_{\text{Zn}}\text{Tz}-8\text{P}_{\text{FB}}$ was fitted by two time components 7.4 (71%) and 1.3 (29%) ns, indicating the energy transfer efficiency is lower than those of $\text{P}_{\text{Zn}}\text{Tz}-2\text{P}_{\text{FB}}$ and $\text{P}_{\text{Zn}}\text{Tz}-4\text{P}_{\text{FB}}$ due to the increased distance between P_{Zn} and P_{FB} s by the additional hydroxymethyl benzyl linker in $\text{P}_{\text{Zn}}\text{Tz}-8\text{P}_{\text{FB}}$ (Figure 5 and Table 4).

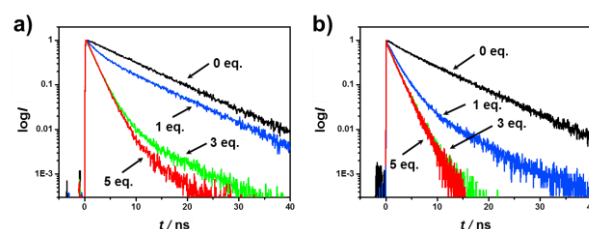


Figure 4. Time-resolved fluorescence decay profiles of $\text{P}_{\text{Zn}}\text{Tz}-2\text{P}_{\text{FB}}$ (2.0 μM) in CH_2Cl_2 upon the addition of CN^- (0, 1, 3, 5 eq.). Each decay profiles were monitored at 700 nm with photoexcitation at a) 400 nm and b) 445 nm.

Table 3. Best-fit parameters of the fluorescence decay profiles of $\text{P}_{\text{Zn}}\text{Tz}-2\text{P}_{\text{FB}}$ ^[a] with various concentration of titrated CN^- ^[b] in CH_2Cl_2 .

[CN^-] ^[b]	400 ^[c]		445	
	τ_1 / ns	τ_2 / ns	τ_1 / ns	τ_2 / ns
0	8.20	n.d. ^[c]	7.80	n.d.
1	8.19 (51%)	2.04 (49%)	6.8 (11%)	1.80 (89%)
3	7.45 (2%)	1.70 (98%)	n.d. ^[c]	1.73
5	7.50 (1%)	1.73 (99%)	n.d.	1.75

[a] The concentration was 2.0 μM . [b] [CN^-]/[$\text{P}_{\text{Zn}}\text{Tz}-2\text{P}_{\text{FB}}$] = 0, 1, 3, 5. [c] λ_{ex} / nm. [d] Not detected. Relative errors of τ values are less than ± 0.06 ps.

By addition of CN^- to $\text{P}_{\text{Zn}}\text{Tz}-n\text{P}_{\text{FB}}$, intriguing features were observed in a series of fluorescence decay profiles. An additional short decay component of about 1.7 ns was observed upon the addition of CN^- to $\text{P}_{\text{Zn}}\text{Tz}-2\text{P}_{\text{FB}}$ (Figure 4 and Table 3). Because this lifetime constant was consistent

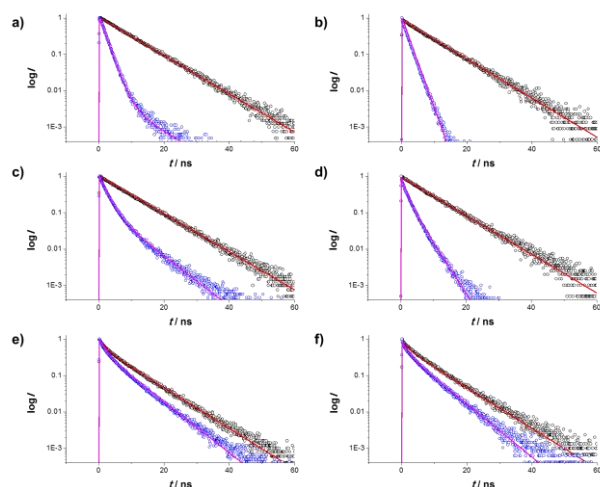


Figure 5. Time-resolved fluorescence decay profiles of a-b) $P_{Zn}Tz-2P_{FB}$ (2.0 μM), c-d) $P_{Zn}Tz-4P_{FB}$ (1.0 μM), and e-f) $P_{Zn}Tz-8P_{FB}$ (0.5 μM) with (blue circle) and without (black circle) 10 eq. CN^- addition in CH_2Cl_2 . Each decay profiles were monitored at 630 nm with photoexcitation at a, c, e) 400 nm and b, d, f) 445 nm.

Table 4. Best-fit parameters of the fluorescence decay profiles of $P_{Zn}Tz-nP_{FB}$ with and without 10 eq. CN^- addition in CH_2Cl_2 .

	400 ^[a]		445	
	τ_1 / ns	τ_2 / ns	τ_1 / ns	τ_2 / ns
$P_{Zn}Tz-2P_{FB}$	8.2	n.d. ^[b]	8.2	n.d.
$P_{Zn}Tz-2P_{FB} + CN^-$	6.5 (1%)	1.7 (99%)	n.d.	1.7
$P_{Zn}Tz-4P_{FB}$	8.3	n.d.	8.3	n.d.
$P_{Zn}Tz-4P_{FB} + CN^-$	6.5 (14%)	2.0 (86%)	4.8 (8%)	1.9 (92%)
$P_{Zn}Tz-8P_{FB}$	7.4 (71%)	1.9 (29%)	7.4 (72%)	1.9 (28%)
$P_{Zn}Tz-8P_{FB} + CN^-$	4.7 (40%)	1.6 (60%)	4.3 (51%)	1.2 (49%)

[a] λ_{ex} / nm. [b] not detected.

with that of $P_{Zn}Tz$, we presumed that this newly observed fast decay component originated from the focal P_{Zn} moiety. Therefore, it can be again inferred that anionic binding of the P_{Zn} moiety with CN^- lowers the lowest energy state of P_{Zn} , leading to a reversal in the direction of intramolecular energy transfer. Moreover, as the concentration of CN^- was increased, the short-lifetime component became dominant, eventually reaching 99% for the addition of 5 eq CN^- . Similarly, the fluorescence decay component of 1.9 ns became predominant with 10 eq. of CN^- addition to $P_{Zn}Tz-4P_{FB}$ (Figure 5 and Table 4). Consequently, we concluded that the coordination of CN^- to the focal P_{Zn} almost completely reversed the energy transfer direction. In the case of $P_{Zn}Tz-8P_{FB}$, the ratio of short lifetime component increased by addition of CN^- (Figure 5 and Table 4). As aforementioned, the energy transfer efficiency from P_{Zn} to P_{FB} moieties in $P_{Zn}Tz-8P_{FB}$ was relatively lower than those of $P_{Zn}Tz-2P_{FB}$ and $P_{Zn}Tz-4P_{FB}$ due to the increased distance from P_{Zn} to P_{FB} s in $P_{Zn}Tz-8P_{FB}$. Therefore, the efficiency of reverse directional energy transfer from P_{FB} moieties to the focal P_{Zn}

would also be lower than those of $P_{Zn}Tz-2P_{FB}$ and $P_{Zn}Tz-4P_{FB}$. Although the energy transfer efficiency of $P_{Zn}Tz-8P_{FB}$ was not as greatly high as that of $P_{Zn}Tz-2P_{FB}$ and $P_{Zn}Tz-4P_{FB}$, the directional control of energy transfer was observed within porphyrin-based artificial light harvesting dendrimer.

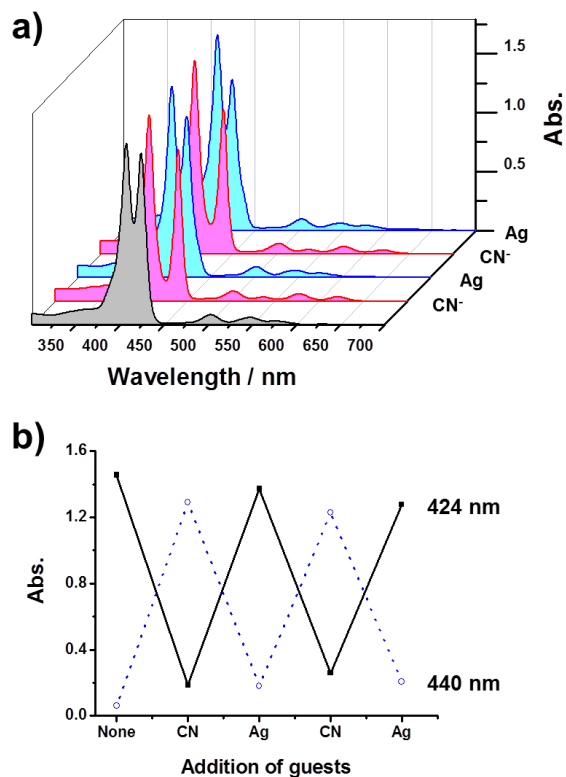


Figure 6. Absorption changes of $P_{Zn}Tz-2P_{FB}$ by treatment with CN^- and silver strip. a) UV/Vis spectral changes, b) absorption monitored at 424 nm (black, solid line) and 440 nm (blue, dotted line).

The energy transfer direction in $P_{Zn}Tz-nP_{FB}$ can be controlled in a reversible manner. Initially, the excitation energy in $P_{Zn}Tz-nP_{FB}$ flows from the focal P_{Zn} to the P_{FB} wings. After the addition of CN^- , the excitation energy of P_{FB} wings flows to the focal P_{Zn} . Owing to the high affinity of silver to CN^- , we could remove CN^- from the solution by treating with a silver strip. The changes in the absorption spectra of $P_{Zn}Tz-2P_{FB}$ observed after CN^- addition were reversed after subsequent treatment with silver (Figure 6); the effect on fluorescence emission was similar (Figure S7). Therefore, the energy transfer direction in $P_{Zn}Tz-2P_{FB}$ can be reversibly controlled by treatment with CN^- and silver.

Conclusion

As a mimicry of light harvesting antenna, we have designed multi-porphyrin dendrimers comprising a triazole-bearing focal zinc porphyrin with a different number of freebase porphyrin wings. By addition of various anionic guest, we could control HOMO-LUMO gap of the focal zinc porphyrin. Therefore, the energy transfer pathway in

the artificial light harvesting dendrimer could be modulated by guest bindings. Such a guest-induced modulation of energy transfer pathway possibly provides a new strategy toward molecular-based photonic switch or molecular machinery.

ASSOCIATED CONTENT

Supporting Information. Synthetic procedures and additional spectral data (Figures S1–8). This material is available free of charge via the Internet at <http://pubs.acs.org>.

AUTHOR INFORMATION

Corresponding Author

wdjang@yonsei.ac.kr
dongho@yonsei.ac.kr

Present Address

†J.S.: Department of Chemistry, University of Oxford, Oxford OX1 3QZ, U.K.

Notes

The authors declare no competing financial interest.

ACKNOWLEDGMENT

This work was supported by the Mid-Career Researcher Program (2014R1A2A1A10051083), Global Research Laboratory Program (2013K1A1A2A02050183) funded by the National Research Foundation (NRF) of Korea, Ministry of Science, ICT & Future, and the Korea Institute of Energy Technology Evaluation and Planning (KETEP) and the Ministry of Trade, Industry & Energy (MOTIE) of the Republic of Korea (No. 20163030013960). The quantum calculations were performed using the supercomputing resources of the Korea Institute of Science and Technology Information (KISTI).

REFERENCES

- Barber, J. *Chem. Soc. Rev.* **2009**, *38*, 185.
- Cheng, Y. C.; Fleming, G. R. *Annu. Rev. Phys. Chem.* **2009**, *60*, 241.
- Scholes, G. D.; Fleming, G. R.; Olaya-Castro, A.; van Grondelle, R. *Nat. Chem.* **2011**, *3*, 763.
- Standfuss, J.; van Scheltinga, A. C. T.; Lamborghini, M.; Kühlbrandt, W. *EMBO J.* **2005**, *24*, 919.
- McConnell, I.; Li, G.; Brudvig, G. W. *Chem. Biol.* **2010**, *17*, 434.
- Kühlbrandt, W.; Wang, D. N. *Nature* **1991**, *350*, 130.
- Duffy, C.; Valkunas, L.; Ruban, A. *Phys. Chem. Chem. Phys.* **2013**, *15*, 18752.
- Joo, T.; Jia, Y.; Yu, J.-Y.; Jonas, D. M.; Fleming, G. R. *J. Phys. Chem.* **1996**, *100*, 2399.
- Kc, C. B.; Stranius, K.; D'Souza, P.; Subbaiyan, N. K.; Lemmetyinen, H.; Tkachenko, N. V.; D'Souza, F. J. *Phys. Chem. C* **2013**, *117*, 763.
- Balaban, T. S. *Acc. Chem. Res.* **2005**, *38*, 612.
- Aratani, N.; Kim, D.; Osuka, A. *Acc. Chem. Res.* **2009**, *42*, 1922.
- Hasobe, T.; Kamat, P. V.; Troiani, V.; Solladie, N.; Ahn, T. K.; Kim, S. K.; Kim, D.; Kongkanand, A.; Kuwabata, S.; Fukuzumi, S. *J. Phys. Chem. B* **2005**, *109*, 19.
- Kim, J. H.; Lee, M.; Lee, J. S.; Park, C. B. *Angew. Chem. Int. Ed.* **2012**, *51*, 517.
- Jeong, Y.-H.; Son, M.; Yoon, H.; Kim, P.; Lee, D.-H.; Kim, D.; Jang, W.-D. *Angew. Chem. Int. Ed.* **2014**, *53*, 6925.
- Li, W.-S.; Aida, T. *Chem. Rev.* **2009**, *109*, 6047.
- Lin, V.; DiMugno, S. G.; Therien, M. J. *Science* **1994**, *264*, 1105.
- Hasobe, T.; Kashiwagi, Y.; Absalom, M. A.; Sly, J.; Hosomizu, K.; Crossley, M. J.; Imahori, H.; Kamat, P. V.; Fukuzumi, S. *Adv. Mater.* **2004**, *16*, 975.
- Hasobe, T.; Imahori, H.; Kamat, P. V.; Ahn, T. K.; Kim, S. K.; Kim, D.; Fujimoto, A.; Hirakawa, T.; Fukuzumi, S. *J. Am. Chem. Soc.* **2005**, *127*, 1216.
- Martinez-Diaz, M. V.; de la Torre, G.; Torres, T. *Chem. Commun.* **2010**, *46*, 7090.
- Li, J. Z.; Ambroise, A.; Yang, S. I.; Diers, J. R.; Seth, J.; Wack, C. R.; Bocian, D. F.; Holten, D.; Lindsey, J. S. *J. Am. Chem. Soc.* **1999**, *121*, 8927.
- Lupton, J.; Samuel, I. D.; Frampton, M.; Beavington, R.; Burn, P. *Adv. Funct. Mater.* **2001**, *11*, 287.
- Ideta, R.; Tasaka, F.; Jang, W.-D.; Nishiyama, N.; Zhang, G.-D.; Harada, A.; Yanagi, Y.; Tamaki, Y.; Aida, T.; Kataoka, K. *Nano Lett.* **2005**, *5*, 2426.
- Nishiyama, N.; Iriyama, A.; Jang, W.-D.; Miyata, K.; Itaka, K.; Inoue, Y.; Takahashi, H.; Yanagi, Y.; Tamaki, Y.; Koyama, H. *Nat. Mater.* **2005**, *4*, 934.
- Jang, W.-D.; Selim, K. K.; Lee, C.-H.; Kang, I.-K. *Prog. Polym. Sci.* **2009**, *34*, 1.
- Son, K. J.; Yoon, H. J.; Kim, J. H.; Jang, W.-D.; Lee, Y.; Koh, W. G. *Angew. Chem. Int. Ed.* **2011**, *50*, 11968.
- Yoon, H.-J.; Lim, T. G.; Kim, J.-H.; Cho, Y. M.; Kim, Y. S.; Chung, U. S.; Kim, J. H.; Choi, B. W.; Koh, W.-G.; Jang, W.-D. *Biomacromolecules* **2014**, *15*, 1382.
- Burke, J.; Ditto, C.; Arntzen, C. *Arch. Biochem. Biophys.* **1978**, *187*, 252.
- Grossman, A. R.; Schaefer, M. R.; Chiang, G. G.; Collier, J. L. *Microbiol. Rev.* **1993**, *57*, 725.
- Nelson, N.; Ben-Shem, A. *Nat. Rev. Mol. Cell Biol.* **2004**, *5*, 971.
- Yoon, H.; Lim, J. M.; Gee, H.-C.; Lee, C.-H.; Jeong, Y.-H.; Kim, D.; Jang, W.-D. *J. Am. Chem. Soc.* **2014**, *136*, 1672.
- Frisch, M. J.; Trucks, G. W.; Schlegel, H. B.; Scuseria, G. E.; Robb, M. A.; Cheeseman, J. R.; Scalmani, G.; Barone, V.; Mennucci, B.; Petersson, G. A.; Nakatsuji, H.; Caricato, M.; Li, X.; Hratchian, H. P.; Izmaylov, A. F.; Bloino, J.; Zheng, G.; Sonnenberg, J. L.; Hada, M.; Ehara, M.; Toyota, K.; Fukuda, R.; Hasegawa, J.; Ishida, M.; Nakajima, T.; Honda, Y.; Kitao, O.; Nakai, H.; Vreven, T.; Montgomery Jr., J. A.; Peralta, J. E.; Ogliaro, F.; Bearpark, M. J.; Heyd, J.; Brothers, E. N.; Kudin, K. N.; Staroverov, V. N.; Kobayashi, R.; Normand, J.; Raghavachari, K.; Rendell, A. P.; Burant, J. C.; Iyengar, S. S.; Tomasi, J.; Cossi, M.; Rega, N.; Millam, N. J.; Klene, M.; Knox, J. E.; Cross, J. B.; Bakken, V.; Adamo, C.; Jaramillo, J.; Gomperts, R.; Stratmann, R. E.; Yazyev, O.; Austin, A. J.; Cammi, R.; Pomelli, C.; Ochterski, J. W.; Martin, R. L.; Morokuma, K.; Zakrzewski, V. G.; Voth, G. A.; Salvador, P.; Dannenberg, J. J.; Dapprich, S.; Daniels, A. D.; Farkas, Ö.; Foresman, J. B.; Ortiz, J. V.; Cioslowski, J.; Fox, D. J.; Gaussian, Inc.: Wallingford, CT, USA, 2009.
- Becke, A. D. *J. Chem. Phys.* **1993**, *98*, 5648.
- Lee, C.; Yang, W.; Parr, R. G. *Phys. Rev. B* **1988**, *37*, 785.
- Kim, D.; Heo, J.; Ham, S.; Yoo, H.; Lee, C.-H.; Yoon, H.; Ryu, D.; Kim, D.; Jang, W.-D. *Chem. Commun.* **2011**, *47*, 2405.
- Yoon, H.; Lee, C.-H.; Jeong, Y.-H.; Gee, H.-C.; Jang, W.-D. *Chem. Commun.* **2012**, *48*, 5109.
- Lee, C. H.; Lee, S.; Yoon, H.; Jang, W. D. *Chem. Eur. J.* **2011**, *17*, 13898.
- Jang, W.-D.; Jeong, Y.-H. *Supramol. Chem.* **2013**, *25*, 34.
- Hua, Y.; Flood, A. H. *Chem. Soc. Rev.* **2010**, *39*, 1262.
- Nappa, M.; Valentine, J. S. *J. Am. Chem. Soc.* **1978**, *100*, 5075.
- Zhang, Y.; Oh, J.; Wang, K.; Chen, C.; Cao, W.; Park, K. H.; Kim, D.; Jiang, J. *Chem. Eur. J.* **2016**, *22*, 4492.

